Inorganica Chimica Acta 437 (2015) 74–80

Contents lists available at ScienceDirect

Inorganica Chimica Acta

journal homepage: www.elsevier.com/locate/ica

Syntheses, structures and properties of a series of hetero-nuclear clusters between transition metals and rare-earth metals based on amino acid

Qing Wang, Bao Mu, Lei Lv, Dan-Dan Yang, Ru-Dan Huang *

Key Laboratory of Cluster Science of Ministry of Education, School of Chemistry, Beijing Institute of Technology, Beijing 100081, PR China

ARTICLE INFO

Article history:
Received 19 July 2015
Accepted 20 August 2015
Available online 28 August 2015

Keywords:
Heteronuclear clusters
Coordination complex
Solvothermal reaction
Amino acid
Luminescent property

ABSTRACT

Six high-heteronuclear clusters, consisting of transition metals and rare-earth metals, have been prepared via the solvothermal reaction, with the formula $[\text{LnNi}_6(\textbf{LTP})_{12}]\cdot3(\text{NO}_3)$ (Ln = La·**1**, Ce·**2**, Pr·**3**, Nd·**4**, Sm·**5**, Gd·**6**, **LTP** = L-thioproline). Complexes **1**–**6** can be described as hepta-nuclear hetero-clusters. The IR spectra, elemental analyses, thermal analyses, XRD and single-crystal X-ray diffraction of **1**–**6** have been measured. X-ray single-crystal structural analyses indicate that **1**–**6** are isomorphic with the triclinic $P\bar{1}$ space group. A twelve-coordinated Ln^{3+} ion is located in the center of a distorted octahedron. Each vertex of the octahedron is situated by a six-coordinated Ni^{2+} ion. **LTP** plays an important role in linking the Ln^{3+} ion and the Ni^{2+} ion. Furthermore, luminescent properties of the title complexes have been investigated at room temperature, and the results indicate that these complexes may be act as the potential materials applied in the fluorescent field.

1. Introduction

More and more attention has been focused on the polynuclear complexes based on transition metals [1–3] or rare-earth metals [4–7], because of the fascinating structures and the interesting properties, such as photochemistry [8–10], magnetism [11,12], catalysis [13]. An accumulating number of researches on metal–organic frameworks based on transition metals or rare-earth metals have been reported [14–20]. Because of the different properties between transition metals and rare-earth metals, it is hard to get the mixed metal complexes. As the research continued, various synthetic routes have been put forward to obtain hetero-nuclear complexes containing transition metal ions and rare-earth metal ions [21–29]. According to the statistics contemporarily, there are a considerable number of reports on complexes $\{\text{LnM}_n\}$ (M = Cu, Ni, Co), In which the most Ln^{3+} ions prefer to be nine-coordinated [21–23,27,28].

Many factors could influence the assemble process of metal–organic complexes, especially, the nature of organic ligands. Amino acid are acted as an important biological ligand and has been widely used [1,21], such as glycine, L-proline. Owing that amino acid is consisted of carboxylate groups and amino groups, it is likely to coordinate lanthanoid ions and transition ions. A series of f–d clusters consisted with glycine have been synthesized and characterized by Wu's group [24,28]. For **LTP** (as show in Chart 1), it is an effective antineoplastic amino acid, the initial study of which is from 1980s [30–32]. And it has an advantageous in coordination by adjusting the twisting angle, so that the flexibility of **LTP** is outperform than the L-proline and glycine. In our previous work [33], the interaction between transition metal ions and amino acid containing sulfur atom have been researched. Three novel homochiral helical MOFs have been synthesized with **LTP** via self-assembly process. In this paper, a series of hetero-metal high-clusters $[\text{LnNi}_6(\textbf{LTP})_{12}]\cdot3(\text{NO}_3)$ have been prepared and characterized. Recently, further study on the coordination chemistry of transition metals and lanthanides with amino acids is also going on.

2. Material and physical measurements

All chemical reagents were purchased commercially and used without further purification. Elemental analyses (C, H, N) were taken on a Perkin–Elmer 2400 CHN elemental analyzer. IR spectra (using KBr pellets) were recorded on a Nicolet 170SX spectrophotometer. Thermogravimetric analyses (TGA) were performed with a heating rate of 10 °C/min using a Exstar SII TG/DTA 7200 integration thermal analyzer. Powder X-ray diffraction (PXRD)

---

* Corresponding author.
E-mail address: huangrd@bit.edu.cn (R.-D. Huang).

http://dx.doi.org/10.1016/j.ica.2015.08.010
0020-1693/© 2015 Elsevier B.V. All rights reserved.

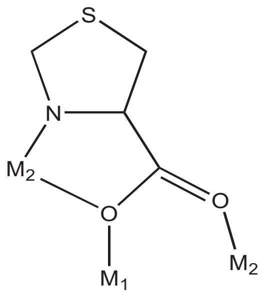

Chart 1. Coordination modes for **LTP**.

was measured on a Siemens D5005 diffractometer (Cu Kα radiation, λ = 1.5410 Å) in the 2θ = 5–50° range. Luminescent spectra were performed with a Hitachi F-4600 fluorescence/phosphorescence spectrophotometer at room temperature.

2.1. X-ray diffraction analysis

Single-crystal X-ray diffraction data were collected on a Bruker APEX diffractometer equipped with a graphite-monochromated Mo Kα (λ = 0.71073 Å) radiation using an ω scan mode at 293 K for **1** and **3**–**5**, at 298 K for **2** and **6**. The structures of **1**–**6** were solved by direct methods using SHELXTL crystallographic software package and refined by the full-matrix least-squares methods on F^2 with SHELXL. A summary of the crystallographic data of **1**–**6** are listed in Table 1. Selected bond lengths and bond angles are given in Tables S1–S6.

2.2. Preparation of the complexes

2.2.1. Synthesis of [LaNi$_6$(*LTP*)$_{12}$]·3(NO$_3$) (*1*)

$La(NO_3)_3 \cdot 6H_2O$ (0.25 mmol, 0.108 g), $Ni(NO_3)_2 \cdot 6H_2O$ (0.25 mmol, 0.073 g) and **LTP** (0.25 mmol, 0.075 g) were added to a mix solution of DMF/ethanol (v/v = 2:1) in a 25 ml Teflon-lined autoclave. After stirring for 20 min, the mixture was keep at 100 °C for 3 days and then cooled to room temperature. Purple ribbed crystals of **La**·**1** were obtained in the final product. (Yield: 41.3% based on **LTP**). Elemental analyses (%) calcd for $C_{48}H_{72}LaN_{15}Ni_6O_{33}S_{12}$: C, 25.45; H, 3.18; N, 9.28; found: C, 25.42; H, 3.15; N, 9.32. IR data (KBr pellet, cm^{-1}): 3432(m), 3280(w), 3169(m), 2908(w), 1627(s), 1587(s), 1424(s), 1384(s), 1321(s), 1283(w), 1223(m), 1159(m), 1093(m), 1005(m), 938(s), 898(m), 837(m), 747(s), 644(m), 574(m).

2.2.2. Synthesis of [CeNi$_6$(*LTP*)$_{12}$]·3(NO$_3$) (*2*)

The complex **2** was synthesized with the similar procedure as **La**·**1**, except that $La(NO_3)_3 \cdot 6H_2O$ (0.25 mmol, 0.108 g) was replaced by $Ce(NO_3)_3 \cdot 6H_2O$ (0.25 mmol, 0.109 g). Purple ribbed crystals of **Ce**·**2** were obtained in the final product. (Yield: 34.7% based on **LTP**). Elemental analyses (%) calcd for $C_{48}H_{72}CeN_{15}Ni_6O_{33}S_{12}$: C, 25.42; H, 3.18; N, 9.27; found: C, 25.38; H, 3.17; N, 9.24. IR data (KBr pellet, cm^{-1}): 3435(m), 3290(w), 3172(m), 2905(w), 1619 (s), 1591(s), 1425(s), 1383(s), 1322(s), 1286(w), 1220(m), 1158 (m), 1087(m), 1006(m), 942(s), 896(m), 837(m), 747(s), 646(m), 570(m).

2.2.3. Synthesis of [PrNi$_6$(*LTP*)$_{12}$]·3(NO$_3$) (*3*)

The complex **3** was synthesized with the similar procedure as **La**·**1**, except that $La(NO_3) \cdot 6H_2O$ (0.25 mmol, 0.108 g) was replaced by $Pr(NO_3)_3 \cdot 6H_2O$ (0.25 mmol, 0.109 g). Purple ribbed crystals of **Pr**·**3** were obtained in the final product. (Yield: 40.3% based on **LTP**). Elemental analyses (%) calcd for $C_{48}H_{72}PrN_{15}Ni_6O_{33}S_{12}$: C, 25.43; H, 3.18; N, 9.27; found: C, 25.46; H, 3.21; N, 9.31. IR data (KBr pellet, cm^{-1}): 3434(m), 3292(w), 3182(m), 2909(w), 1619(s), 1589(s), 1424(s), 1383(s), 1322(s), 1284(w), 1218(w), 1157(m), 1090(m), 1007(m), 938(s), 896(m), 838(m), 750(s), 650(m), 570(m).

2.2.4. Synthesis of [NdNi$_6$(*LTP*)$_{12}$]·3(NO$_3$) (*4*)

The complex **4** was synthesized with the similar procedure as **La**·**1**, except that $La(NO_3)_3 \cdot 6H_2O$ (0.25 mmol, 0.108 g) was replaced by $Nd(NO_3)_3 \cdot 6H_2O$ (0.25 mmol, 0.110 g). Royal purple ribbed crystals of **Nd**·**4** were obtained in the final product. (Yield: 35.7% based on **LTP**). Elemental analyses (%) calcd for $C_{48}H_{72}NdN_{15}Ni_6O_{33}S_{12}$: C, 25.39; H, 3.17; N, 9.26; found: C, 25.45; H, 3.12; N, 9.19. IR data (KBr pellet, cm^{-1}): 3436(m), 3295(w), 3187(m), 2914(w), 1620 (s), 1591(s), 1425(s), 1383(s), 1325(s), 1287(w), 1220(w), 1158 (m), 1072(m), 1006(m), 940(s), 898(m), 837(m), 753(s), 646(m), 573(m).

2.2.5. Synthesis of [SmNi$_6$(*LTP*)$_{12}$]·3(NO$_3$) (*5*)

The complex **5** was synthesized with the similar procedure as **La**·**1**, except that $La(NO_3)_3 \cdot 6H_2O$ (0.25 mmol, 0.108 g) was replaced by $Sm(NO_3)_3 \cdot 6H_2O$ (0.25 mmol, 0.112 g). Royal purple ribbed crystals of **Sm**·**5** were obtained in the final product. (Yield: 38.5% based on **LTP**). Elemental analyses (%) calcd for $C_{48}H_{72}SmN_{15}Ni_6O_{33}S_{12}$: C, 25.32; H, 3.17; N, 9.23; found: C, 25.30; H, 3.15; N, 9.28. IR data (KBr pellet, cm^{-1}): 3435(m), 3293(w), 3185(m), 2917(w), 1619 (s), 1590(s), 1425(s), 1385(s), 1325(s), 1284(w), 1222(w), 1158 (m), 1076(m), 1006(m), 940(s), 899(m), 837(m), 752(s), 645(m), 574(m).

2.2.6. Synthesis of [GdNi$_6$(*LTP*)$_{12}$]·3(NO$_3$) (*6*)

The complex **6** was synthesized with the similar method to that of **La**·**1**, except that $La(NO_3)_3 \cdot 6H_2O$ (0.25 mmol, 0.108 g) was replaced by $Gd(NO_3)_3 \cdot 6H_2O$ (0.25 mmol, 0.113 g). Royal purple ribbed crystals of **Gd**·**6** were obtained in the final product. (Yield: 28.4% based on **LTP**). Elemental analyses (%) calcd for $C_{48}H_{72}SmN_{15}Ni_6O_{33}S_{12}$: C, 25.25; H, 3.16; N, 9.20; found: C, 25.31; H, 3.18; N, 9.16. IR data (KBr pellet, cm^{-1}): 3435(m), 3296(w), 3195 (w), 2922(m), 1623(s), 1586(s), 1405(s), 1381(s), 1322(s), 1286 (w), 1220(w), 1157(m), 1103(w), 1005(m), 940(s), 896(m), 834 (m), 747(s), 646(m), 573(m).

3. Results and discussion

3.1. Crystal structure description

X-ray structural analyses show that complexes **1**–**6** are isomorphous and crystallized in the triclinic $P\bar{1}$ space group. As a representative example, the crystal structure of **1** was described in detail. The asymmetric unit of **1** contains one unique La^{3+} ion, six unique Ni^{2+} ions, twelve **LTP** ligands and three NO_3^- ions. As shown in Fig. 1a, that the structure formed by six Ni^{2+} ions is a large distorted octahedron with the La^{3+} ion in the center.

The La^{3+} ion is coordinated by twelve O atoms from carboxylic groups of twelve **LTP** ligands, which is a distorted $\{LaO_{12}\}$ icosahedral coordination conformation, as depicted in Fig. 2b. The La–O bond lengths vary from 2.687(13) to 2.741 (12) Å (Table 2) and the O–La–O bond angles are in the range of 61.9(4)–180.0(2). Each Ni^{2+} ion is linking to two N atoms from two **LTP** ligands and four O atoms from four different **LTP** ligands, which is described as a distorted $\{NiO_4N_2\}$ octahedron coordination conformation (Fig. 2d). In the octahedron, two N atoms and two O atoms of the **LTP** are placed in four equatorial sites. And the other two O atoms of the **LTP** are lying in the axial sites. The distance between the Ni^{2+} ion and the adjacent N ion is among 2.080 Å and 2.125 Å, the length of Ni–O is between 2.005(15) Å and 2.079(15) Å, which have been